Cyclic Voltammetry of Rh(I) Complexes and the Oligomers. A Correlation between the Anodic Peak Potentials and the Rate Constants for the Electron Transfer Reactions with Inorganic Oxidants

Shunichi Fukuzumi, Nobuaki Nishizawa, and Toshio Tanaka*

Department of Applied Chemistry, Faculty of Engineering, Osaka University, Suita, Osaka 565

(Received February 5, 1982)

The cyclic voltammogram of a CH_3CN solution of $[Rh(p\text{-}MeOC_6H_4NC)_4]^+$ exhibits three anodic current peaks which correspond to the oxidations of the monomer, the dimer, and the trimer, with no cathodic wave on the reverse scan. The anodic peak potentials E^p_{ox} in such irreversible cyclic voltammograms were determined for various Rh(I) monomers and the oligomers such as $[Rh(RNC)_4]^+$, $[Rh_2(RNC)_8]^{2+}$, $[Rh_2(dppm)_2(RNC)_4]^{2+}$, $[Rh_2(dicp)_4]^{2+}$, $[Rh_3(RNC)_{12}]^{3+}$, and $[Rh_4(dicp)_8]^{4+}$ (R=*p*-$MeOC_6H_4$ and Ph, *etc*; dppm=bis(diphenylphosphino)methane, dicp=1,3-diisocyanopropane). The anodic peak potentials E^p_{ox} vary mainly with the degree of oligomerization of the Rh(I) complexes, decreasing in the order monomer>dimer>trimer>tetramer, in parallel with the energies of the highest occupied molecular orbitals E_{HOMO}. It has been found that the E^p_{ox} values are linearly correlated with logarithm of the rate constants for the electron transfer reactions with inorganic oxidants such as $[Fe(bpy)_3]^{3+}$ and $[Co(bpy)_3]^{3+}$ (bpy=2,2′-bipyridine) in the context of the Marcus theory as expected when the standard oxidation potentials E^0_{ox} would be used. It is thus suggested that the anodic peak potentials of the Rh(I) complexes in the irreversible system can be used as the standard oxidation potentials as far as the relative values are concerned.

Recently, Rh(I) complex oligomers such as $[Rh_2(dicp)_4]^{2+}$ (dicp=1,3-diisocyanopropane) have merited a special attention since Gray *et al.*[1] discovered that $[Rh_2(dicp)_4]^{2+}$ dissolved in 12 mol dm^{-3} aqueous HCl solution produces H_2 upon irradiation of visible light. It seems to be of importance to know the redox properties of the Rh(I) complexes in order to delineate the mechanism as well as to improve the efficacy of the system. However, the redox properties of Rh(I) complexes have scarcely been known in contrast with other conventional systems of photosensitized hydrogen production such as utilizing $[Ru(bpy)_3]^{2+}$ (bpy=2,2′-bipyridine)[2-4] whose redox properties have well been established.[5]

Previously, we have reported the kinetic study on the electron transfer reactions of tetrakis(isocyanide)-rhodium(I) and the oligomers, $[(RhL_4^+)_n]$ (n=1—3), with inorganic oxidants such as $[Fe(N\text{-}N)_3]^{3+}$ (N-N= 2,2′-bipyridine, 1,10-phenanthroline, and related ligands) and $[Co(bpy)_3]^{3+}$,[6] in which $[(RhL_4^+)_n]$ were found to undergo irreversible oxidation by these oxidants. In such irreversible systems, the thermodynamic redox properties of $[(RhL_4^+)_n]$ such as the redox potentials E^0 cannot be obtained directly. It seems, however, to be possible to relate the dynamic properties of $[(RhL_4^+)_n]$ in the redox reactions to the redox potential by utilizing the linear free energy relationship (LFER).

In the present study, we wish to report the relation between the dynamic properties of various Rh(I) complexes including $[Rh_2(dicp)_4]^{2+}$ in the electrochemical oxidation, obtained as the anodic peak potentials of the cyclic voltammograms (E^p_{ox}), and the standard oxidation potentials of the complexes (E^0_{ox}), by comparing the E^p_{ox} values with the electron transfer rate constants for the reactions with inorganic oxidants (k_1) reported previously.[6] It will be shown that the anodic peak potentials (E^p_{ox}) provide useful informations on the differences between the redox properties of the Rh(I) monomers and the oligomers.

Experimental

Materials. Preparations of tetrakis(isocyanide)rhodium(I) perchlorates used in this study were described previously.[6,7] Bis(diphenylphosphino)methane (dppm) was prepared according to the literature.[8] dppm-Bridged Rh(I) dimers of the $[Rh_2(dppm)_2(RNC)_4]^{2+}$ type (R=Ph, *p*-$MeOC_6H_4$, *t*-Bu, $PhCH_2$) were prepared by adding a stoichiometric amount of dppm to a solution of appropriate $[Rh(RNC)_4](ClO_4)$ in acetone by the procedure analogous to the preparation of $[Rh_2(dppm)_2(n\text{-}BuNC)_4]^{2+}$.[9] The product was collected by filtration and purified by recrystallization from acetone/ethanol, followed by drying in a vacuum. The elemental analysis was performed for a representative compound, $[Rh_2(dppm)_2(p\text{-}MeOC_6H_4NC)_4](ClO_4)_2$. Found: C, 57.25; H, 4.56; N, 3.23%. Calcd for $Rh_2C_{82}H_{72}N_4P_4Cl_2O_{12}$: C, 57.73; H, 4.25; N, 3.28%. 1,3-Diisocyanopropane (dicp) was prepared from 1,3-propanediamine, chloroform, and 50% aqueous sodium hydroxide by the procedure analogous to the preparation of phenyl isocyanide,[10] and the product was purified by vacuum distillation. The dicp-bridged Rh(I) dimer, $[Rh_2(dicp)_4]Cl_2$, was prepared by the reaction of dicp with $[Rh(cyclooctadiene)Cl]_2$[11] in chloroform according to the literature.[12] The tetraphenylborate salt, $[Rh_2(dicp)_4](BPh_4)_2$, was obtained by the addition of $NaBPh_4$ to a methanol solution of $[Rh_2(dicp)_4]Cl_2$. Tetrabutylammonium perchlorate used as a supporting electrolyte was prepared by the reaction of tetrabutylammonium bromide with perchloric acid, and purified by recrystallization from ethanol. Acetonitrile used as a solvent for electrochemical and kinetic experiments was purified by the standard method.[13]

Cyclic Voltammetry. Cyclic voltammetry measurements were performed on a Hokuto Denko Model HA-301 potentiostat/galvanostat at 298 K in CH_3CN containing 0.1 mol dm^{-3} n-Bu_4NClO_4 as a supporting electrolyte, using a platinum microelectrode and a standard NaCl calomel reference electrode (SCE) or a Ag/Ag^+ reference electrode ($Ag/AgNO_3$ 0.1 mol dm^{-3}). The electrochemical cell was constructed according to the literature.[14] The platinum microelectrode was routinely cleaned by soaking it in concentrated nitric acid, followed by repeated rinsing with water

and then acetone, and drying at 353 K prior to use. Two cm³ of a CH_3CN solution of Rh(I) complexes (1.0×10^{-3}—1.0×10^{-2} mol dm^{-3}) was introduced into the cell and flashed with nitrogen prior to the measurements. The anodic peak potentials, E^p_{ox}, observed at the same sweep rate of 100 mV s^{-1} for the Rh(I) complexes employed in this study were always reproducible to within 50 mV. No aging of the electrode was observed on a week to week basis. There were no complications on the electrode arising from the deposition of the oxidized Rh(II) species for most Rh(I) complexes so that the repeated scans did not affect the appearance of the voltammograms. For some Rh(I) dimer complexes such as $[Rh_2(dicp)_4]^{2+}$ and $[Rh_2(dppm)_2(t\text{-BuNC})_4]^{2+}$, the anodic peak current decreased with repeating the scan, but the anodic peak potentials in the first scan were reproducible. The cyclic voltammetry of $[Rh_2(dicp)_4]^{2+}$ was measured in a methanol solution of the chloride salt containing 0.04 mol dm^{-3} KCl or 0.1 mol dm^{-3} LiCl, since the salt was not soluble enough in CH_3CN containing 0.1 mol dm^{-3} n-Bu_4NClO_4. The anodic peak potential of each Rh(I) complex in CH_3CN containing 0.1 mol dm^{-3} n-Bu_4NClO_4 *vs.* Ag/Ag$^+$ (Ag/AgNO$_3$ 0.1 mol dm^{-3}) was 0.34 V lower than that *vs.* SCE. The same difference between the redox potentials of ferrocene used as a reference compound *vs.* Ag/Ag$^+$ and SCE was always observed in accordance with the literature.[15]

Kinetic Measurements of Electron Transfer Reactions. The measurements of rates of the electron transfer reactions between Rh(I) complexes and $[Fe(N\text{-}N)_3]^{3+}$ were described previously.[6] Rates of the electron transfer reactions between dppm-bridged Rh(I) complexes, $[Rh_2(dppm)_2(RNC)_4]^{2+}$, and $[Co(bpy)_3]^{3+}$ in CH_3CN were measured at 298 K by monitoring the decay of the absorbances due to the Rh(I) dimers (λ_{max} listed in Table 1) in the presence of large excess $[Co(bpy)_3]^{3+}$ (2.19×10^{-3}—1.22×10^{-2} mol dm^{-3}), by using a Union SM-401 spectrophotometer. A mixing apparatus (Model MX-7, Union Giken) was used to ensure the fast and complete mixing of the two sample solutions. The ionic strength of the reaction medium was adjusted to 0.1 with n-Bu_4NClO_4.

Results

Cyclic Voltammetry of Rh(I) Complexes. The cyclic voltammograms (CV) of three representative Rh(I) complexes, $[Rh(p\text{-}MeOC_6H_4NC)_4]^+$, $[Rh(2,4,6\text{-}Me_3C_6H_2NC)_4]^+$, and $[Rh_2(dppm)_2(PhNC)_4]^{2+}$, are illustrated in Fig. 1, which shows anodic waves with current maxima but no cathodic wave on the reverse scan, as confirmed by changing the sweep rates in the range 20 mV s^{-1} to 1000 mV s^{-1}. The anodic oxidation of the Rh(I) complexes is thus irreversible, indicating that the follow-up chemical reactions are fast on the time scale of the CV experiments.

The CV of $[Rh(p\text{-}MeOC_6H_4NC)_4]^+$ shows three distinct anodic current peaks in the range 0.2—1.2 V *vs.* Ag/Ag$^+$ (Fig. 1a), which correspond to the fact that the $[Rh(p\text{-}MeOC_6H_4NC)_4]^+$ cation oligomerizes in CH_3CN to exist as an equilibrium mixture with the dimer $[Rh_2(p\text{-}MeOC_6H_4NC)_8]^{2+}$ and the trimer $[Rh_3(p\text{-}MeOC_6H_4NC)_{12}]^{3+}$, as shown in Eqs. 1 and 2,[6,16]

$$2[RhL_4]^+ \overset{K_D}{\rightleftharpoons} [Rh_2L_8]^{2+} \quad (1)$$

$$[Rh_2L_8]^{2+} + [RhL_4]^+ \overset{K_T}{\rightleftharpoons} [Rh_3L_{12}]^{3+} \quad (2)$$

where L represents p-$MeOC_6H_4NC$. Similar multi-

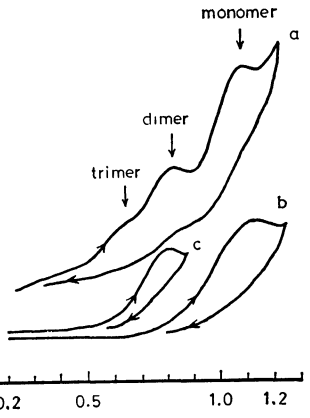

Fig. 1. Cyclic voltammograms of representative Rh(I) complexes in CH_3CN containing 0.1 mol dm^{-3} n-Bu_4NClO_4; (a) $[Rh(p\text{-}MeOC_6H_4NC)_4]^+$ 2.1×10^{-2} mol dm^{-3}, (b) $[Rh(2,4,6\text{-}Me_3C_6H_2NC)_4]^+$ 1.0×10^{-3} mol dm^{-3}, (c) $[Rh_2(dppm)_2(PhNC)_4]^{2+}$ 5.1×10^{-3} mol dm^{-3}.

CV peaks were observed for $[Rh(p\text{-}MeC_6H_4NC)_4]^+$ and $[Rh(PhNC)_4]^+$ which also are known to oligomerize in CH_3CN.[6,17] On the other hand, $[Rh(2,4,6\text{-}Me_3C_6H_2NC)_4]^+$ does not oligomerize appreciably because of the steric effect of the bulky ligand,[6] and there exists only the monomer as the predominant species in CH_3CN, *e.g.*, 99.9% monomer in 2.21×10^{-3} mol dm^{-3} where the CV was measured. Indeed, the CV of $[Rh(2,4,6\text{-}Me_3C_6H_2NC)_4]^+$ shows a single anodic current peak at 1.14 V (Fig. 1b) which is nearly the same as the position of the third anodic peak for $[Rh(p\text{-}MeOC_6H_4NC)_4]^+$. Similar single CV peaks were observed for $[Rh(C_6H_{11}NC)_4]^+$, $[Rh(2,6\text{-}Me_2C_6H_3NC)_4]^+$, $[Rh(t\text{-BuNC})_4]^+$, and $[Rh(PhCH_2NC)_4]^+$ which do not oligomerize appreciably either.[6] dppm-Bridged Rh(I) dimers of the $[Rh_2(dppm)_2(RNC)_4]^{2+}$ type (R=Ph, $PhCH_2$, t-Bu) do not oligomerize in CH_3CN either.[9] In accordance with this, the CV of $[Rh_2(dppm)_2(PhNC)_4]^{2+}$ exhibits a single anodic wave due to the oxidation of the dimer with a current maximum at 0.68 V (Fig. 1c) which corresponds to the second anodic peak of $[Rh(p\text{-}MeOC_6H_4NC)_4]^+$.

Based on the above results, the three anodic current peaks at 1.03, 0.79, and 0.56 V for the CV of $[Rh(p\text{-}MeOC_6H_4NC)_4]^+$ can be assigned to the oxidation of the monomer, the dimer, and the trimer, respectively. Anodic peak potentials E^p_{ox} of Rh(I) complexes determined at the same sweep rate (100 mV s^{-1}) are listed in Table 1. The peak potentials E^p_{ox} of the Rh(I) monomers (Nos. 1—8) are approximately constant, independent of the nature of isocyanide ligands. Those values of the Rh(I) dimers present in CH_3CN solutions of $[RhL_4]^+$ (Nos. 9—11) also are constant at 0.76±0.03 V, but smaller by about 0.3 V than the Rh(I) monomers. Moreover, the E^p_{ox} values (Nos. 12—15) are slightly smaller than those of the Rh(I) dimers whose ligands are not bridged. The $[Rh_2(dicp)_4]^{2+}$ cation partly oligomerizes to form the tetramer in methanol (Eq. 3). The formation of the

$$2[Rh_2(dicp)_4]^{2+} \overset{K_D}{\rightleftharpoons} [Rh_4(dicp)_8]^{4+} \quad (3)$$

Table 1. Anodic peak potentials of CV for Rh(I) complexes (E^{p}_{ox})[a] and the electronic absorption maxima (λ_{max} and $h\nu_{max}$)

No.	Monomer	E^{p}_{ox} *vs.* Ag/Ag$^+$ V	λ_{max} nm	$h\nu_{max}$ eV
1	$[Rh(p\text{-}MeOC_6H_4NC)_4]^+$	1.03±0.01	403	3.08
2	$[Rh(p\text{-}MeC_6H_4NC)_4]^+$	1.06±0.02	407	3.05
3	$[Rh(PhNC)_4]^+$	1.18±0.02	411	3.02
4	$[Rh(2,4,6\text{-}Me_3C_6H_2NC)_4]^+$	1.14±0.04	405	3.06
5	$[Rh(C_6H_{11}NC)_4]^+$	1.09±0.01	385	3.22
6	$[Rh(2,6\text{-}Me_2C_6H_3NC)_4]^+$	1.03±0.02	409	3.03
7	$[Rh(t\text{-}BuNC)_4]^+$	1.20±0.01	383	3.24
8	$[Rh(PhCH_2NC)_4]^+$ Dimer	1.07±0.04	387	3.20
9	$[Rh_2(p\text{-}MeOC_6H_4NC)_8]^{2+}$	0.79±0.02	564	2.20
10	$[Rh_2(p\text{-}MeC_6H_4NC)_8]^{2+}$	0.74±0.04	563	2.20
11	$[Rh_2(PhNC)_8]^{2+}$	0.76±0.01	568	2.18
12	$[Rh_2(dppm)_2(PhNC)_4]^{2+}$	0.68±0.01	613	2.02
13	$[Rh_2(dppm)_2(PhCH_2NC)_4]^{2+}$	0.62±0.02	548	2.26
14	$[Rh_2(dppm)_2(t\text{-}BuNC)_4]^{2+}$	0.63±0.01	526	2.36
15	$[Rh_2(dicp)_4]^{2+}$ Trimer	0.58±0.02[b]	559[b]	2.22[b]
16	$[Rh_3(p\text{-}MeOC_6H_4NC)_{12}]^{3+}$ Tetramer	0.56±0.02	710	1.75
17	$[Rh_4(dicp)_8]^{4+}$	0.25±0.04[b]	778[b]	1.59[b]

a) Measured at the sweep rate of 100 mV s^{-1} in CH_3CN containing 0.1 mol dm^{-3} n-Bu_4NClO_4 at 298 K unless otherwise noted. b) Measured in methanol containing 0.04 mol dm^{-3} KCl.

tetramer, $[Rh_4(dicp)_8]^{4+}$, is characterized by the appearance of a new absorption band at 778 nm in the high concentrations in addition to absorption bands at 318, 342, and 559 nm observed in the low concentrations. The anodic current peak which is assignable to the tetramer appears at the smallest potential (No. 17) among the Rh(I) complexes in Table 1. Thus, the E^{p}_{ox} values for the Rh(I) monomers and the oligomers in Table 1 are concluded to increase in the order tetramer < trimer < dimer(bridged) < dimer(not bridged) < monomer.

Electron Transfer Reactions of Rh(I) Complexes with Inorganic Oxidants. The kinetics of the oxidation of Rh(I) monomers, $[Rh(RNC)_4]^+$, with inorganic oxidants such as $[Fe(N\text{-}N)_3]^{3+}$ (Eq. 4) were examined earlier,[6]

$$[RhL_4]^+ + [Fe(N\text{-}N)_3]^{3+} \longrightarrow [RhL_4]^{2+} + [Fe(N\text{-}N)_3]^{2+} \quad (4)$$

where N-N=2,2′-bipyridine, 1,10-phenanthroline, and substituted 1,10-phenanthrolines. The kinetic results in the presence of excess oxidants were best interpreted by the scheme,[6]

$$[RhL_4]^+ + Ox \overset{K_1}{\rightleftharpoons} ([RhL_4]^+\ Ox) \xrightarrow{k_1} \text{e. t.} \quad (5)$$

$$([RhL_4]^+\ Ox) + Ox \overset{K_2}{\rightleftharpoons} ([RhL_4]^+\ 2Ox) \xrightarrow{k_2} \text{e. t.} \quad (6)$$

Scheme

where Ox and e.t. represent the inorganic oxidants and the electron transfer reactions as the rate determining step, respectively. In order to compare the reactivity of Rh(I) dimers with Rh(I) monomers, the electron transfer reactions of $[Rh_2(dppm)_2(RNC)_4]^{2+}$ with $[Co(bpy)_3]^{3+}$ were examined kinetically in CH_3CN containing 0.1 mol dm^{-3} n-Bu_4NClO_4 at 298 K. The reactions were followed by monitoring the decay of the absorbance due to $[Rh_2(dppm)_2(RNC)_4]^{2+}$ (λ_{max} in Table 1).[18] The reactions obey pseudo-first-order kinetics in the presence of excess $[Co(bpy)_3]^{3+}$. According to the Scheme the pseudo-first-order rate constant k_{Co} is expressed as

$$k_{Co} = \frac{k_1K_1[Co] + k_2K_1K_2[Co]^2}{1 + K_1[Co] + K_1K_2[Co]^2} \quad (7)$$

When $K_1[Co] \gg 1$ and $K_2[Co] \ll 1$, Eq. 7 is reduced to Eq. 8.

$$k_{Co} = k_1 + k_2K_2[Co] \quad (8)$$

The plots of k_{Co} *vs.* [Co] are given in Fig. 2, which shows linear relations, in accordance with Eq. 8. The intramolecular electron transfer rate constant k_1 in Eq. 5 can thus be obtained from the extrapolated intercepts in Fig. 2 (compare with Eq. 8). The plot of k_{Fe} *vs.* [Fe] for the electron transfer reaction of $[Rh(PhCH_2NC)_4]^+$ with $[Fe(N\text{-}N)_3]^{3+}$ also is shown in Fig. 2 for comparison. The k_1 values for the reactions of Rh(I) complexes with $[Co(bpy)_3]^{3+}$ as well as $[Fe(N\text{-}N)_3]^{3+}$ are listed in Table 2, which gives the difference between the anodic peak potentials of Rh(I) complexes, E^{p}_{ox}, (Table 1) and the reduction potentials of the oxidants, E^{0}_{red},[6] as well for comparison. It can be seen that the electron transfer rate constants k_1 vary significantly from 1.0×10^{-6} to 1.2×10^{2} s^{-1}, approximately in parallel with the $E^{p}_{ox}-E^{0}_{red}$ values.

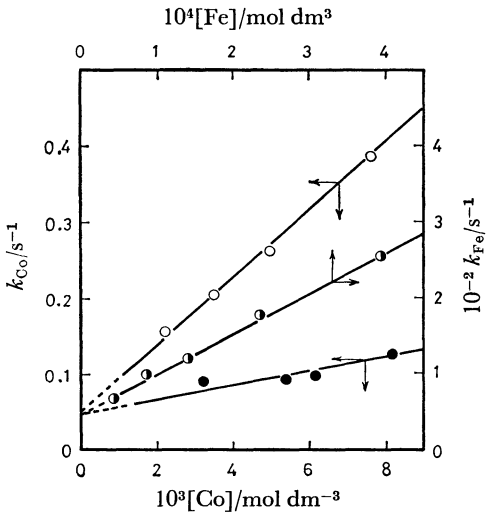

Fig. 2. Pseudo-first-order rate constants k_{Co} and k_{Fe} as a function of [Co] or [Fe] for the oxidations of $[Rh_2(dppm)_2(p\text{-}MeOC_6H_4NC)_4]^{2+}$ (○) and $[Rh_2(dppm)_2(PhCH_2NC)_4]^{2+}$ (●) with $[Co(bpy)_3]^{3+}$ and of $[Rh(PhCH_2NC)_4]^+$ (◑) with $[Fe(bpy)_3]^{3+}$, respectively, in CH_3CN containing 0.1 mol dm^{-3} n-Bu_4NClO_4 at 298 K.

Discussion

Peak Potentials of CV in Irreversible Systems. In

Table 2. Electron transfer rate constants k_1 for the reactions of Rh(I) complexes with $[Co(bpy)_3]^{3+}$ and $[Fe(N\text{-}N)_3]^{3+}$.[a]

Rh No.[b]	Oxidant	$E^p_{ox}-E^0_{red}$[c] / V	k_1[d] / s^{-1}	Rh No.[b]	Oxidant	$E^p_{ox}-E^0_{red}$[c] / V	k_1[d] / s^{-1}
Monomer				Monomer			
1	$[Fe(bpy)_3]^{3+}$	0.31	1.2×10^2	7	$[Fe(bpy)_3]^{3+}$	0.48	5.0
2	$[Fe(bpy)_3]^{3+}$	0.34	3.4×10		$[Fe(phen)_3]^{3+}$	0.47	4.0×10
	$[Fe(phen)_3]^{3+}$	0.33	4.6×10		$[Fe(5\text{-}Clphen)_3]^{3+}$	0.38	3.8×10
3	$[Fe(bpy)_3]^{3+}$	0.46	5.0×10		$[Fe(5\text{-}NO_2phen)_3]^{3+}$	0.27	3.8×10
	$[Fe(phen)_3]^{3+}$	0.45	3.2×10	8	$[Fe(bpy)_3]^{3+}$	0.35	4.3×10
4	$[Co(bpy)_3]^{3+}$	1.17	1.0×10^{-6}		$[Fe(phen)_3]^{3+}$	0.34	4.6×10
	$[Fe(4,7\text{-}Ph_2phen)_3]^{3+}$	0.47	4.6	Dimer			
	$[Fe(bpy)_3]^{3+}$	0.42	2.7	9	$[Co(bpy)_3]^{3+}$	0.82	
	$[Fe(phen)_3]^{3+}$	0.41	2.0×10	10	$[Co(bpy)_3]^{3+}$	0.77	1.5×10^{-3}
	$[Fe(5\text{-}Clphen)_3]^{3+}$	0.31	1.3×10	11	$[Co(bpy)_3]^{3+}$	0.79	1.6×10^{-3}
	$[Fe(5\text{-}NO_2phen)_3]^{3+}$	0.21	1.1×10^2	12	$[Co(bpy)_3]^{3+}$	0.71	8.2×10^{-2}[e]
5	$[Fe(bpy)_3]^{3+}$	0.37	4.3×10	13	$[Co(bpy)_3]^{3+}$	0.65	6.3×10^{-2}[e]
	$[Fe(phen)_3]^{3+}$	0.36	4.6×10	14	$[Co(bpy)_3]^{3+}$	0.66	
6	$[Fe(bpy)_3]^{3+}$	0.31	8.6×10	Trimer			
	$[Fe(phen)_3]^{3+}$	0.30	9.4×10	16	$[Co(bpy)_3]^{3+}$	0.59	5.4×10^{-1}
7	$[Co(bpy)_3]^{3+}$	1.23	1.5×10^{-6}	Tetramer			
	$[Fe(4,7\text{-}Ph_2phen)_3]^{3+}$	0.53	3.5	17	$[Co(bpy)_3]^{3+}$	0.28	

a) In CH_3CN containing 0.1 mol dm^{-3} n-Bu_4NClO_4 at 298 K. b) Numbers refer to compounds in Table 1. c) The E^0_{red} values are taken from Ref. 6. d) From Ref. 6 unless otherwise noted. e) This study.

reversible systems, an anodic current peak potential of CV is thermodynamically determined and the corresponding cathodic peak is observed in the reverse scan with the peak separation of 59 mV, irrespective of the sweep rate.[19] Thus, the redox potential E^0 is experimentally determined as $(E^p_{ox}+E^p_{red})/2$. When the oxidized species is unstable, however, the CV becomes irreversible since the oxidized species no longer exists on the electrode owing to the facile chemical reactions. Under such circumstances, the redox potential cannot be determined, and the anodic peak potential is dependent on a number of factors such as the electron transfer rate constant on the electrode, the reverse electron transfer rate constant, the sweep rate of the CV, and the rate constants of the follow-up chemical reactions. Recently, Klingler and Kochi[20] have, however, demonstrated that under the conditions where the follow-up chemical reactions are much faster than the reverse electron transfer, the anodic peak potential becomes independent of the follow-up chemical reactions since the forward electron transfer is the rate determining step. The anodic peak potential E^p_{ox} is then expressed in terms of the oxidation potential E^0_{ox}, the transfer coefficient β, and the electron transfer rate constants $k(E^p_{ox})$ and $k(E^0_{ox})$ at the peak potential and the oxidation potential, respectively,[20,21]

$$E^p_{ox} = E^0_{ox} + \frac{RT}{\beta F}\ln\frac{k(E^p_{ox})}{k(E^0_{ox})} \quad (9)$$

where $k(E^p_{ox})$ (in units of cm s^{-1}) is a function of the sweep rate v (in V s^{-1}) as given by Eq. 10,[19]

$$k(E^p_{ox}) = 2.18(D\beta Fv/RT)^{1/2} \quad (10)$$

where D (in cm^2 s^{-1}) is the diffusion coefficient and the other notations are conventional. It should be noted that the diffusion coefficient D is nearly constant irrespective of metal complexes.[20] Thus, if β and $k(E^0_{ox})$ are constant, the peak potential E^p_{ox} is linearly related to the standard oxidation potential E^0_{ox} with the slope of unity at a constant sweep rate as given by Eq. 11. Under such conditions, the peak potential

$$E^p_{ox} = E^0_{ox} + \text{Const.} \quad (11)$$

E^p_{ox} can be used as the thermodynamically defined oxidation potential E^0_{ox} as far as the relative values are concerned. In order to examine whether Eq. 11 is applicable to the anodic oxidation of Rh(I) complexes, the irreversibility of the CV wave is discussed in the following section.

Irreversibility in Oxidation of Rh(I) Complexes. The CV of Rh(I) complexes in Fig. 1 clearly demonstrates that the anodic oxidation of Rh(I) complexes is irreversible since no cathodic wave is observed in the reverse scan at the sweep rate as high as 1000 mV s^{-1}. The oxidized Rh(I) complexes, *i.e.*, Rh(II) species have well been regarded as radicals,[6,22] and dimerize rapidly (Eq. 12). An additional support for the irreversibility

$$2[RhL_4]^{2+} \xrightarrow{\text{fast}} [Rh_2L_8]^{4+} \quad (12)$$

in the anodic oxidation of Rh(I) complexes is given by the sweep rate dependence of the anodic peak potential E^p_{ox}. By combining Eqs. 9 and 10, one obtains Eq. 13 which shows that E^p_{ox} depends on the sweep rate v,[20]

$$E^p_{ox} = \frac{2.3RT}{2\beta F}\log v + \text{Const.} \quad (13)$$

where

$$\text{Const.} = E^0_{ox} + \frac{2.3RT}{\beta F}\log\frac{2.18D\beta F}{k(E^0_{ox})RT} \quad (14)$$

In Fig. 3, the E^p_{ox} values for some representative Rh(I) complexes are plotted against logarithm of the sweep rates. A linear correlation is obtained for each

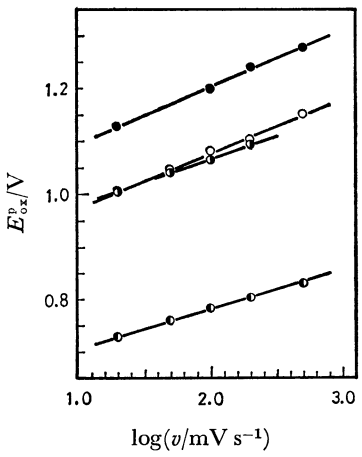

Fig. 3. Anodic peak potentials E^p_{ox} of $[Rh(t\text{-}BuNC)_4]^+$ (●), $[Rh(C_6H_{11}NC)_4]^+$ (○), $[Rh(p\text{-}MeOC_6H_4NC)_4]^+$ (◑), and $[Rh_2(p\text{-}MeOC_6H_4NC)_8]^{2+}$ (◐) as a function of the CV sweep rate v at a platinum microelectrode in CH_3CN containing 0.1 mol dm^{-3} n-Bu_4NClO_4 at 298 K.

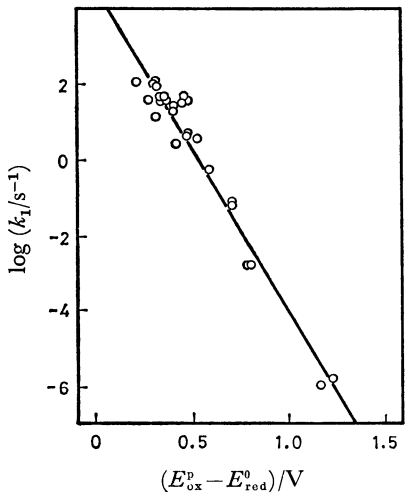

Fig. 4. Correlation between log k_1 for the oxidations of Rh(I) complexes with inorganic oxidants in CH_3CN and $E^p_{ox}-E^0_{red}$. Compare with Eq. 18 in text.

Rh(I) complex in accordance with Eq. 13. The slopes in Fig. 3 are almost the same for the present Rh(I) complexes, as 95±10 mV per decade, and are significantly larger than those of partially reversible electron transfer between the limits of 0 and 30 mV per decade.[19] Such large slopes may be characteristic of totally irreversible processes. Thus, from Eq. 13 the transfer coefficient β is obtained as 0.31±0.04 for the Rh(I) complexes studied here. The same β value was obtained from the analysis of the half-width of the CV wave in Fig. 1 by the use of Eq. 15 as well,[19]

$$E^p_{ox} - E^{p/2}_{ox} = 1.857\ (RT/\beta F) \quad (15)$$

where $E^{p/2}_{ox}$ represents the electrode potential at the half peak current.

A Linear Free Energy Relationship (LFER) in the Irreversible Oxidation of Rh(I) Complexes. The foregoing section has established the conditions to use the E^p_{ox} values as the relative E^0_{ox} values (Eq. 11), such as the total irreversibility and the constant transfer coefficient β. In order to test the validity of Eq. 11 for the oxidation of Rh(I) complexes independently, the E^p_{ox} values have been compared with the electron transfer rate constants k_1 for the chemical oxidations of the Rh(I) complexes with inorganic oxidants by the following manner. Previously, the intramolecular electron transfer rate constants k_1 for reactions of a given Rh(I) complex with a series of inorganic oxidants whose reduction is reversible have been related to the reduction potentials of the oxidants by Eq. 16,[6] which accords with the Marcus relation (Eq. 17),[23]

$$\log k_1 = 8.5E^0_{red} + \text{Const.} \quad (16)$$

$$\log k_1 = -8.5\Delta G^0 + \text{Const.} \quad (17)$$

where ΔG^0 is the standard free energy change of electron transfer reactions given by $E^0_{ox}-E^0_{red}$ (in V). If Eq. 11 can be applied to the oxidations of Rh(I) complexes, the E^0_{ox} values which cannot be determined directly may be substituted by the experimentally accessible values of E^p_{ox}, and Eq. 17 is rewritten as Eq. 18. The relation of Eq. 18 is tested by plotting

$$\log k_1 = -8.5\ (E^p_{ox}-E^0_{red}) + \text{Const.} \quad (18)$$

the log k_1 values for the oxidations of Rh(I) complexes with the inorganic oxidants against the $(E^p_{ox}-E^0_{red})$ values by taking the data in Table 2, as shown in Fig. 4. There is seen an excellent agreement between the experimental plot in Fig. 4 and the relation in Eq. 18 (the slope is −8.6 with the correlation coefficient ρ=0.98), which strongly supports the validity of Eq. 11. Thus, the LFER in Fig. 4 underscores the utility of the anodic peak potentials E^p_{ox} at a constant sweep rate for obtaining the relative oxidation potentials E^0_{ox} of Rh(I) complexes.

Variation of HOMO with Rh(I) Oligomerization. The E^p_{ox} values of Rh(I) complexes vary with the Rh(I) oligomerization (Table 1). Such variations of the E^p_{ox} value must reflect the change of the energy of the highest occupied molecular orbital (HOMO) from which electron is removed upon oxidation since the E^p_{ox} values are related to the standard oxidation potentials E^0_{ox} as discussed in the foregoing section. The variation of the E^p_{ox} values with the Rh(I) oligomerization may be understood by comparing the E^p_{ox} values with the electronic transition energies of the Rh(I) complexes which also reflect the HOMO energies, with the aid of the MO diagram of Rh(I) monomers and the oligomers shown in Fig. 5.[16] The HOMO energy, E^{HOMO}_n (n=1—4), increases with oligomerization, resulting in decrease of the transition energy in the order $h\nu_1 > h\nu_2 > h\nu_3 > h\nu_4$. Thus, the approximate relation between $h\nu_n$ and E^{HOMO}_n is given by Eq. 19 derived from the energy diagram (Fig. 5),

$$h\nu_n = -2E^{HOMO}_n + \text{Const.} \quad (19)$$

where Const. is $h\nu_1+2E^{HOMO}_1$. The E^{HOMO}_n value is related to the oxidation potential E^0_{ox} by Eq. 20,[24]

$$E^{HOMO}_n = -E^0_{ox} + \Delta G^s - C' \quad (20)$$

where ΔG^s is the free energy change of solvation in solutions, and C′ is a constant which includes the potential of the reference electrode on the absolute scale together with the liquid junction potential.[25] When

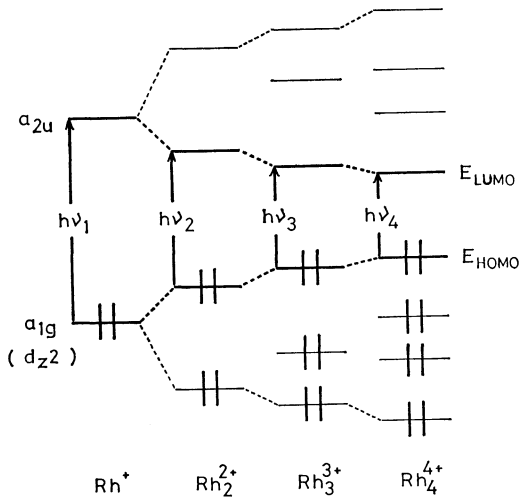

Fig. 5. MO diagram of the Rh(I) monomer and the oligomers.

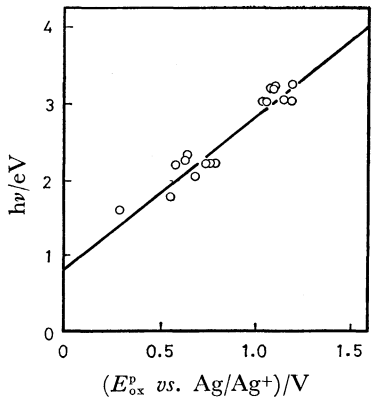

Fig. 6. Correlation between the electronic transition energies $h\nu$ of Rh(I) complexes and the anodic peak potentials E^{p}_{ox}.

ΔG^{s} is assumed as constant in the homologous series of Rh(I) complexes, Eq. 19 is rewritten by Eq. 21. Then, the relation between $h\nu_n$ and the anodic peak potential E^{p}_{ox} is obtained as Eq. 22, by substituting Eq. 11 into Eq. 21. The validity of Eq. 22 is confirmed from the plot between $h\nu$ and E^{p}_{ox} as shown in Fig. 6. Thus, the correlation between $h\nu$ and E^{p}_{ox} gives an additional support for the conclusion that the anodic peak potential E^{p}_{ox} can be taken as the relative thermodynamic quantity for the oxidation of Rh(I) complexes, E^{0}_{ox}, which cannot otherwise be obtained directly.

$$h\nu_n = 2E^{0}_{ox} + \text{Const.} \quad (21)$$

$$h\nu_n = 2E^{p}_{ox} + \text{Const.} \quad (22)$$

References

1) a) K. R. Mann, N. S. Lewis, V. M. Miskowski, D. K. Erwin, G. S. Hammond, and H. B. Gray, *J. Am. Chem. Soc.*, **99**, 5525 (1977); b) A. W. Maverick and H. B. Gray, *Pure Appl. Chem.*, **52**, 2339 (1980); c) H. B. Gray, K. R. Mann, N. S. Lewis, J. A. Thich, and R. M. Richma, *Adv. Chem. Ser.*, **168**, 44 (1978); d) K. R. Mann and H. B. Gray, *ibid.*, **173**, 225 (1979); e) V. M. Miscowski, I. S. Sigal, K. R. Mann, H. B. Gray, S. J. Milder, G. S. Hammond, and P. R. Ryason, *J. Am. Chem. Soc.*, **101**, 4383 (1979); f) I. S. Sigal, K. R. Mann, and H. B. Gray, *ibid.*, **102**, 7252 (1980).

2) K. Kalyanasundaram and M. Grätzel, *Angew. Chem., Int. Ed. Engl.*, **18**, 701 (1979); J. Kiwi, E. Borgarello, E. Pelizzetti, M. Visca, and M. Grätzel, *ibid.*, **19**, 646 (1980); A. Moradpour, E. Amouyal, P. Keller, and H. Kagan, *Nouv. J. Chim.*, **2**, 547 (1978).

3) J. M. Lehn and J. P. Sauvage, *Nouv. J. Chim.*, **1**, 449 (1977); M. Kirch, J. M. Lehn, and J. P. Sauvage, *Helv. Chim. Acta*, **62**, 1345 (1979); P. J. DeLaive, B. P. Sullivan, T. J. Meyer, and D. G. Whitten, *J. Am. Chem. Soc.*, **101**, 4007 (1979).

4) G. M. Brown, B. S. Brunschwig, C. Creutz, J. F. Endicott, and N. Sutin, *J. Am. Chem. Soc.*, **101**, 1298 (1979).

5) C. Creutz and N. Sutin, *Proc. Natl. Acad. Sci. U.S.A.*, **72**, 2858 (1975); N. Sutin and C. Creutz, *Adv. Chem. Ser.*, **168**, 1 (1978); D. G. Whitten, *Acc. Chem. Res.*, **13**, 83 (1980); C. T. Lin, W. Bottcher, M. Chou, C. Creutz, and N. Sutin, *J. Am. Chem. Soc.*, **98**, 6536 (1976).

6) S. Fukuzumi, N. Nishizawa, and T. Tanaka, *Bull. Chem. Soc. Jpn.*, in press.

7) T. Iinuma and T. Tanaka, *Inorg. Chim. Acta*, **49**, 79 (1981).

8) W. Hewertson and H. R. Watson, *J. Chem. Soc.*, **1962**, 1490.

9) A. L. Balch, *J. Am. Chem. Soc.*, **98**, 8049 (1976).

10) W. P. Weber, G. W. Gokel, and I. K. Ugi, *Angew. Chem., Int. Ed. Engl.*, **11**, 530 (1972).

11) J. Chatt, L. M. Vananzi, *J. Chem. Soc.*, **1957**, 4735.

12) N. S. Lewis, K. R. Mann, J. G. Gordon II, and H. B. Gray, *J. Am. Chem. Soc.*, **98**, 7461 (1976); K. Kawakami, M. Okajima, and T. Tanaka, *Bull. Chem. Soc. Jpn.*, **51**, 2327 (1978).

13) D. D. Perrin, W. L. F. Armarego, and D. R. Perrin, "Purification of Laboratory Chemicals," Pergamon Press, New York (1966).

14) R. P. Van Duyne and C. N. Reilley, *Anal. Chem.*, **44**, 142 (1972).

15) C. K. Mann, *Electroanal. Chem.*, **3**, 57 (1969).

16) K. Kawakami, M. Haga, and T. Tanaka, *J. Organomet. Chem.*, **60**, 363 (1973); K. R. Mann, J. G. Gordon II, and H. B. Gray, *J. Am. Chem. Soc.*, **97**, 3553 (1975); K. R. Mann, N. S. Lewis, R. M. Williams, H. B. Gray, and J. G. Gordon II, *Inorg. Chem.*, **17**, 828 (1978).

17) The third anodic current peak at 0.56 V due to the trimer was not observed clearly because of the smaller K_T.[6)]

18) The rates of reactions between $[Rh_2(dppm)_2(RNC)_4]^{2+}$ and $[Fe(N\text{-}N)_3]^{3+}$ also were examined but too fast to be determined by the stopped-flow technique.

19) R. S. Nicholson and I. Shain, *Anal. Chem.*, **36**, 706 (1964).

20) R. J. Klingler and J. K. Kochi, *J. Am. Chem. Soc.*, **102**, 4790 (1980); **103**, 5839 (1981); *J. Phys. Chem.*, **85**, 1731 (1981).

21) The number of electrons transferred in the rate-determining step is taken as unity.[6)]

22) T. L. Kelly and J. F. Endicott, *J. Am. Chem. Soc.*, **94**, 1797 (1972); B. B. Wayland and A. R. Newman, *ibid.*, **101**, 6472 (1979); H. Ogoshi, J. Setsune, and Z. Yoshida, *ibid.*, **99**, 3869 (1977).

23) R. A. Marcus, *Ann. Rev. Phys. Chem.*, **15**, 155 (1964); *J. Phys. Chem.*, **72**, 891 (1968).

24) M. E. Peover, *Electroanal. Chem.*, **2**, 1 (1967); B. Case, "Reactions of Molecules at Electrodes," ed by N. S. Hush, Wiley Interscience, New York (1971), p. 125.

25) R. E. Ballard, *Chem. Phys. Lett.*, **42**, 97 (1976).